by the rate constants, which appear in the expression of the equilibrium constant $K=K_f/K_b$ and thus enter the description of dynamic equilibrium.

VII. THE DENSITY MATRIX AND FRACTIONAL ATOMS

In a similar vein, in the density matrix description every atom of a macroscopic chunk of tungsten under consideration is "prepared" identically and therefore must be in an identical state. Their state is described by the weight factors assigned to the accessible states, which can be grouped into two subgroups, called "crystalline" and "vapor" phases. The weight factors are allowed to be fractional, so long as their sum over all accessible states equals unity. Thus there is nothing conceptually awkward about "a fraction of an atom." The number of atoms in the vapor phase is defined as (mass/atomic weight)×weight factor of being in the vapor phase, and nothing in principle prevents it from being a fractional number. Only the "picture" of an atom as an indestructible sphere no longer holds, not a very severe loss. The same is true of a "completely" dissociated strong electrolyte and a "sparingly soluble" salt and a nearly undissociated water vapor. The incongruity of the extremely low values of the vapor pressure, or solubility, or extremely large values of dissociation constants encountered in the systems of interest in this paper are thus removed in the density matrix description. We may point out in addition that the tungsten vapor and the solution of silver ion present in equilibrium are homogeneous, as required by equilibrium thermodynamics. The density matrix description is that the weight factor of the states of the tungsten atom in vapor phase, located in different parts of space accessible to it, is uniform. The same statement holds for silver ions in solution.

VIII. CONCLUSION

(1) The systems considered in this paper demand that in order for their thermodynamic description to be valid, a fraction of an atom must be a meaningful concept. This concept has been precisely defined.
(2) The quantum statistical description that uses the density matrix gives a consistent meaning to the concept of a fractional atom. Thus the validity of thermodynamics in these systems requires quantum statistics.
(3) The relationship of the time independent equilibrium state of thermodynamics to the quantum statistical description of the equilibrium state is highlighted.
(4) It is stressed that the concept of a dynamic equilibrium is outside the scope of classical thermodynamics.

ACKNOWLEDGMENTS

Stimulating discussions with Professors Gyan Mohan, Rajat Ray, Debi Khan, Satish Joglekar, Kalyan Banerjee, Messers. Avik Ghosh, Avik Chatterjee, and Jishnu and Kaustuv DasGupta are gratefully acknowledged.

[a]Author for Correspondence.

[1]G. N. Lewis and M. Randall, *Thermodynamics* (McGraw-Hill, New York, 1960), Chap. 8, p. 92–93.
[2]T. L. Hill, *Statistical Mechanics* (McGraw-Hill, New York, 1956), Chap. 1.
[3]W. J. Moore, *Physical Chemistry* (Prentice-Hall, Englewood Cliffs, NJ, 1972), Chaps. 8 and 9.
[4]R. C. Tolman, *Principles of Statistical Mechanics* (Oxford U.P., Oxford, 1938), Secs. 77 and 78.
[5]L. D. Landau and E. M. Lifshitz, *Statistical Physics*, 2nd ed. (Addison-Wesley, Reading, MA, 1969), Sec. 5.
[6]L. D. Landau and E. M. Lifshitz, *Quantum Mechanics* (Pergamon, New York, 1977), 3rd ed. (Revised and enlarged), Sec. 1, pp. 3, 5.

Flow profile study using miniature laser-Doppler velocimetry

W. E. Booij, A. de Jongh,[a] and F. F. M. de Mul[a),b)]
University of Twente, Department of Applied Physics, P. O. Box 217, 7500 AE Enschede, The Netherlands

(Received 24 June 1994; accepted 3 March 1995)

We present a physics experiment, in which laser-Doppler velocimetry is used to make first-year university physics students realize that the idealized solutions offered by standard text books seldom are applicable without corrections, which often are numerical. This is demonstrated by carefully measuring and calculating the flow profile in a rectangular pipe. © *1995 American Association of Physics Teachers.*

INTRODUCTION

Most standard undergraduate textbooks heavily focus on problems for idealized situations that can be solved analytically. This is not sufficient when dealing with problems that the students will face later on as physicists in the real world. It is our opinion that the students have to learn how to solve those problems as well. The lack of study material about nonideal situations in text books can partly be compensated by letting students perform experiments in which a well-known analytical solution is only an approximation and a numerical correction to the analytical approach is necessary.

Such a problem is the laminar flow of a liquid in a pipe with a rectangular cross section. In this case the velocity profile can be written as the sum of the Poiseuille profile and correction terms in the form of a series expansion. The actual velocity profile can be measured by means of a laser-Doppler velocimeter and compared with the theoretical profile. The

expression for the flow between two large parallel plates situated close to each other will offer the analytical approximation.

This article deals with such an experiment, using a dual-beam differential laser-Doppler velocimeter and a flow in a rectangular pipe. The measured flow profile can be fitted with the Poiseuille profile together with terms of a series expansion as a correction. The extra terms can be found by solving the Poisson equation. The setup of the experiment was developed for first-year university physics students. For the laser-Doppler measurements a ready-to-use miniature velocimeter, using a diode laser, was applied. Fourier transformation of the time signals is performed on-line using a personal computer. The experiment was designed in such a way that the process of signal-processing and handshaking in the interface between the velocimeter and the computer is made transparent.

THEORY

For the description of a laminar flow profile in a rectangular pipe the Poiseuille law can be used. Denoting the horizontal and vertical half-widths by x_h and x_v, and the corresponding variables by x_1 and x_2, respectively ($-x_h<x_1<+x_h$ and $-x_v<x_2<+x_v$), the profile in the vertical direction can approximately be written:[1]

$$v(x_1,x_2)\approx v(x_2)=\frac{1}{2\eta}\frac{dp}{dz}(x_v^2-x_2^2) \tag{1}$$

where dp/dz is the pressure gradient in the z direction along the pipe and η is the viscosity. In fact, this approximation is only valid in the case of $x_h \gg x_v$, thus describing a flow between two large parallel plates which are relatively close to each other.

In the case of slow viscous flow in a pipe with a rectangular cross section and a constant pressure gradient that generates a rectilinear flow along the pipe, the hydrodynamic equation can be reduced[1] to Poisson's equation. In the Appendix it is shown that this leads to a correction in the form of a series expansion. With these correction terms the complete expression will read

$$v(x_1,x_2)=\frac{1}{2\eta}\frac{dp}{dz}\left(x_v^2-x_2^2+\frac{32x_v^2}{\pi^3}+\sum_{n=0}^{\infty}\frac{(-1)^{n+1}\cosh((2n+1)\pi x_1/2x_v)\cos((2n+1)\pi x_2/2x_v)}{(2n+1)^3\cosh((2n+1)\pi x_h/2x_v)}\right), \tag{2}$$

with $\cosh(x)=[\exp(x)+\exp(-x)]/2$. From this expression it is clear that the actual profile will deviate from the Poiseuille profile, which is given by the first term.

This expression can be used to compare measured and calculated flow profile data in the setup described in the following section.

EXPERIMENT

The technique of laser-Doppler velocimetry can be regarded as well known[2,3] (see Ref. 4 for recent advances). In the last five years one article about the technique has been published in this journal.[5] This article dealt with the measurement of a moving mirror using a Michelson interferometer setup. We may focus on the description of the instrument used with the present experiment.

A few years ago in our department a miniature differential laser-Doppler velocimeter was developed[6] that uses a semiconductor laser as the light source. This cheap, compact, and easy-to-use velocimeter is called MIRA (mini-interfering rays anemometer), and the paramount advantage of the instrument is that it makes accurate velocimetry feasible without alignment problems, often encountered with velocimeters using gas lasers. The overall dimensions of the instrument used in the present experiment are 12×4×4 cm. A smaller version, with a cylindrical shape of 1 cm diameter and 5 cm length, is available as well.

The configuration of the MIRA is simple. A sketch of the instrument can be found in Fig. 1. A semiconductor laser (wavelength $\lambda=790$ nm) is placed directly in front of a gradient-index lens that focuses the beam onto a grating, which splits the beams into two coherent beams. Normally a phase grating is used; as a result, the two first-order beams contain almost all the intensity (about 90%). Two plano-convex achromatic lenses bring the two beams together to form an interference pattern with a very small volume. A photograph of the interference pattern is shown in Fig. 2. The

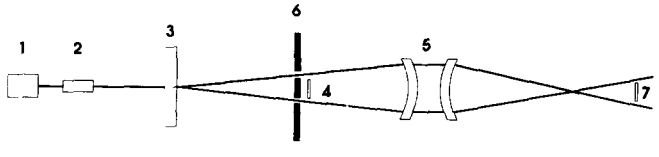

Fig. 1. Scheme of the miniature laser-Doppler velocimeter MIRA [1: diode laser, 2: gradient-index lens, 3: grating, 4: photodiode, 5: achromatic lenses, 6: beam stopper, 7: external photodiode (optional)]. Dimensions of the housing, including 1–6: 12×4×4 cm. Distance from the output lens to the crossing point of the beams: 2–10 cm adjustable.

Fig. 2. Photograph of the interference volume, taken along the optical axis. Fringe spacing: $s=4.6$ μm at $\lambda=800$ nm and $\alpha=10°$.

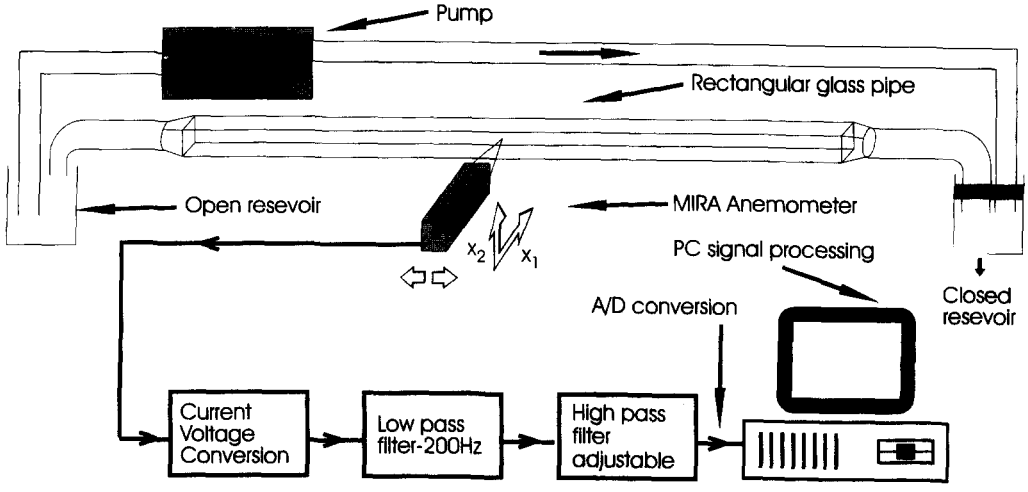

Fig. 3. Total setup of the experiment. Flow pipe: rectangular cross section; glass, $2x_h=20$ mm and $2x_v=20$ mm; length=800 mm with outlets of 50 mm adapting to a tube connection with a diameter of 23 mm.

distance s between two fringes of maximum intensity can be expressed in terms of the wavelength λ of the laser and the angle α between the two coherent beams:

$$s=\lambda/(2\ \sin(\alpha/2)). \tag{3}$$

From the photograph we can conclude that the interference volume has about 24 maxima, so the radius of the interference volume can be calculated provided s is known.

When small particles pass through the interference pattern, laser light will be scattered. The scattering amplitude will depend on the relative refractive index and the shape of the particles. To avoid blurring, the particle size must be smaller than the fringe spacing, and only one particle is allowed to be present in the interference pattern at the same time. Although normally backscattering is far less intense than forward scattering, the MIRA contains a built-in photodiode for detection of the scattered light.

Upon detection the light scattering signal will contain a Doppler beat. The characteristic Doppler frequency f_d depends on the fringe distance s, the angle β between the velocity vector of the particle and the normal on the planes through the fringes, and the velocity of the particle v:

$$f_d=v\ \cos\ \beta/s. \tag{4}$$

The small current signal from the photodiode is converted into a voltage signal and filtered to obtain a good signal-to-noise ratio. A first-order high-pass filter at 200 Hz is used to block the mains frequency. A variable low-pass first-order filter avoids aliasing when the signal is sampled.

In liquids with suspended particles it is very hard to obtain a continuous Doppler frequency signal. To achieve this, on the average one particle always has to be present in the fringe volume. A better way to measure velocity is to use single bursts, arising from a single particle in the fringe volume. The concentration of particles has to be low and in the case of water normal tap water often suffices. In distilled water or other transparent liquids, particles with a diameter in the order of the fringe spacing can be added, e.g., polystyrene spheres, intralipid or TiO_2 particles.

To detect single bursts, we sampled the signal using an AD-converter (Metrabyte DASH 16F with maximum sample frequency of 100 kHz) connected to a personal computer with a 486 processor. The sampling is a continuous background operation so the CPU of the PC can be used to inspect the signal for the occurrence of a burst continuously. A criterion for the acceptance of bursts, that works very well in practice for relatively clean liquids, uses a simple trigger based upon voltage level discrimination. The sample frequency was set at such a value that the burst will fill a sample window of 1024 points in an optimal way.

In a liquid with a suitable concentration of particles, a large number of bursts can be obtained within a few seconds. These time-domain signals are fast Fourier transformed into the frequency domain. Subsequent bursts can be added in this domain in order to improve the accuracy and reliability of the measurement. The Fourier spectrum will clearly show a peak at the Doppler frequency.

In the present instrument the total signal-processing part of the process of sampling and transforming the signal is integrated in a mouse-driven program. This allows the student to focus his or her attention on how to measure and analyze a velocity profile by using laser-Doppler velocimetry as a measuring tool. The program gives the user the opportunity to visually inspect the bursts in the time domain and decide whether the whole or a part of the signal will be used for further processing.

The setup of the experiment is shown in Fig. 3. The flow pipe with rectangular cross section is made of glass, with a reflective back side. This enables the MIRA photodiode to detect forward scattered light. A steady flow is obtained by using a gear pump and a closed flow system with two reservoirs. To scan the profile in the pipe, the MIRA can be moved in three perpendicular directions using translational stages.

The resolution of the velocity profile obtained in this way is limited by the fringe volume of the MIRA. If we assume that the interference pattern is formed by two Gaussian beams with waist w_0, the boundary of the pattern is an ellipsoid with axis lengths a, b, and c given by:

$$a=2w_0,\quad b=2w_0/\cos(\alpha/2),\quad c=2w_0/\sin(\alpha/2), \tag{5}$$

with c measured along the optical symmetry axis, a and b perpendicular to c, and a,b perpendicular and parallel, respectively, to the plane formed by the two beams. We can estimate b by multiplying the number of maxima in a single

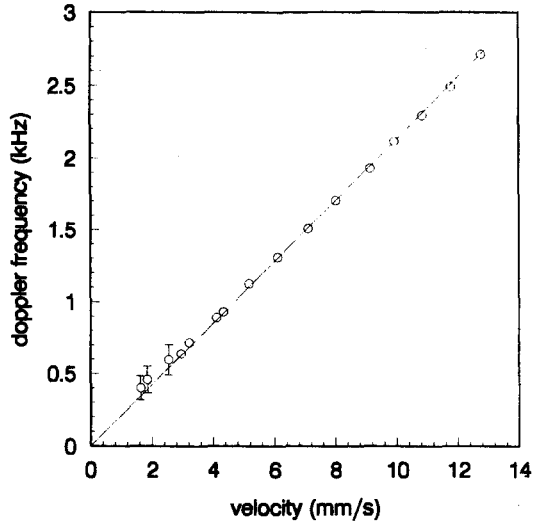

Fig. 4. Relation between the measured frequency and the velocity of a rotation wheel with a least-squares fit (a calibration experiment as an introduction).

burst [14 in Fig. 5(a)] and the fringe distance s. With $s=4.7$ μm this results in $a=66$ μm, $b=66$ μm, and $c=770$ μm.

In the experiments we encountered the problem of reflections of the laser beams into the built-in diode by the reflecting backside of the glass pipe. This caused electronic oversteering of the detector. These reflections can be minimized by rotating the MIRA over a small angle in the horizontal plane. This will have a negligible effect on the measurements.

The Doppler frequency spectrum is calculated by a fast Fourier algorithm, which can be run by the student after each velocity measurement. It is also possible to average over a predefined number of bursts before Fourier transforming the time signals. From the frequency spectrum on the screen the average velocity (with error bar) can be derived, with the help of Eq. (4) [see Figs. 5(a) and 5(b)].

DESIGN OF THE STUDENT EXPERIMENT

In the course of three afternoons, the student is led through the following experiments.

(1) Determine the relationship between the measured frequency and the velocity of the scatterers by using a rotating wheel covered with a piece of paper.

(2a) Measure and interpret velocity profiles half-way along the pipe at a moderate pump rate (laminar flow) and compare these with the theoretical expectations for this flow rate.

(2b) Measure and interpret the velocity profiles, to be measured at the entrance of the pipe and investigate how these profiles deviate from the theoretical profiles.

(2c) Investigate the effects of increasing the velocity beyond the laminar-turbulent transition.

Experiment 1 is an introductory experiment, meant as calibration of the instrument; the velocity of the wheel can be measured independently, and the laser-Doppler frequency from the light scattered by the fibers in the paper can be measured. In experiment 2a the theoretical values will consist of the Poiseuille profile plus the higher-order terms, which ought to be calculated with the help of a computer.

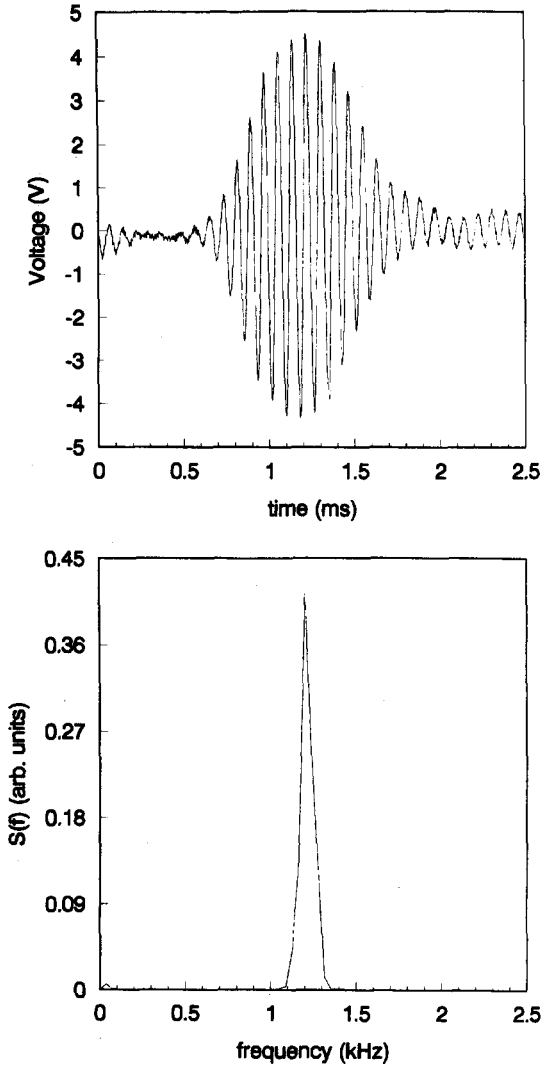

Fig. 5. A burst in the time domain (a) and the frequency domain (b).

These values are compared to the measured profile, as shown in Fig. 6. In experiment 2b the effects of entrance problems will show up and in experiment 2c the Reynolds number may be introduced. Experiment 1 is obligatory; afterwards a choice between 2a, 2b, or 2c can be made.

PERFORMANCE OF THE INSTRUMENT

The Doppler measurements with the rotating wheel (experiment 1) will give the student a good idea of the relationship between the velocity and frequencies involved and of the signal processing. Figure 4 was obtained by averaging ten measurements at several different speeds of the wheel. It can be seen that the relation is linear, as expected. The error in the frequency measurements is mainly determined by the spread in the velocity of the added bursts. For the present instrument the following relationship is obtained:

$$f_d/v=(2.13\pm0.09)\times10^5 \text{ Hz/(m/s)}. \quad (6)$$

An example of a single burst due to scattering of a single particle in the flow is shown in Fig. 5(a). The Fourier transform of this signal shows a clear peak, this being the Doppler frequency [Fig. 5(b)]. For reliable Doppler measurements at a given point in the pipe, a number of these bursts are measured and averaged in the frequency domain. The spread in

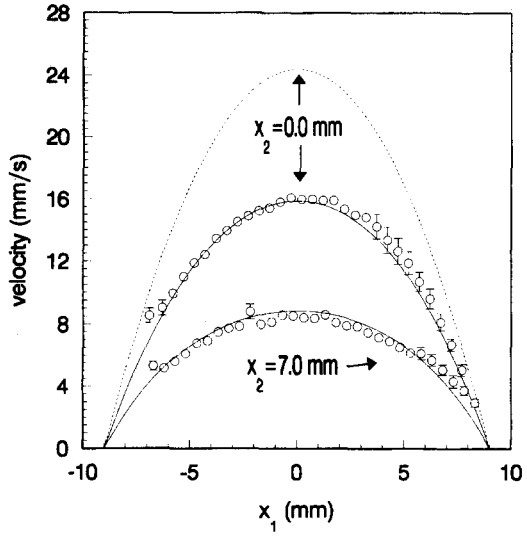

Fig. 6. Velocity profile for $x_2=0.0$ mm and $x_2=7.0$ mm. Dotted line: Poiseuille approximation only; full lines through the measured points: including the correction terms in Eq. (2) up to $n=8$ (convergence up to 92%).

the peak frequencies is due to the steadiness of the flow, the degree of turbulence, or the finite dimensions of the interference pattern.

To illustrate the performance of the instrument, the velocity profiles in the pipe are measured at $x_2=0.0$ mm and $x_2=7.0$ mm by varying x_1. Here at each x_1 position 20 bursts were averaged. The pump rate Φ for these measurements was measured independently, to be 2.73×10^{-6} m^3/s. By measuring the velocity profile over the whole cross section of the pipe we can determine $(dp/dz)/2\eta$ using

$$\Phi=\int_{-x_v}^{+x_v}\int_{-x_h}^{+x_h} v(x_1,x_2)dx_1\,dx_2. \tag{7}$$

In Fig. 6 both the measured velocity profile of the two Doppler measurements as well as the theoretical profile using the value for $(dp/dz)/2\eta$ obtained with the help of Eq. (7) are shown. The correspondence is quite good. The Poiseuille profile is clearly seen to be an approximation only. At higher pump rates the Doppler peak broadens due to turbulence effects.

STUDENT'S IMPRESSIONS

Having developed a setup with which it is easy to measure the Doppler frequencies of suspended particles by "aiming" the MIRA at a specific point in the pipe and waiting for the computer to accomplish its task of gathering Doppler bursts, we felt that the experiment of measuring velocity profiles was within reach of first-year university students in applied physics. We therefore tested this assumption with a number of those students.

The students who have performed this experiment felt that it gave them more insight in the possibilities of the modern measurement techniques and the use of computers in experiments. The experiment was highly recommended by the students.

Prior to the experiments, the students have to become introduced to the relevant theory, consisting of Poiseuille's law and the mathematics of the corrections.

CONCLUSIONS

The velocity profile measured with the MIRA in a pipe with rectangular cross section corresponds to the behavior predicted with the Poiseuille profile and the correcting series expansion. It can be seen by the student that the Poiseuille profile is just an approximation and that the series expansion is needed to obtain a better description of the measured profile.

The experiment gives the student the opportunity to work with modern miniature laser equipment, with software to transform the data into frequency spectra. These frequency spectra have to be transformed into velocity profiles with the help of another computer program. The student will have to interpret these results and compare them with the analytical description.

The computer programs for measuring and interpreting the data are available on request.

ACKNOWLEDGMENTS

The authors thank P. Fornerod and B. Oude Alink for their help in this project.

APPENDIX

In this Appendix a short survey will be given over the way of calculating the correction terms in Eq. (2). A full description can be found in Ref. 11.

We start with the Poisson equation for the velocity in the z direction:

$$\nabla^2 v=\left(\frac{\partial^2}{\partial x_1^2}+\frac{\partial^2}{\partial x_2^2}\right)v=-\frac{1}{\eta}\frac{dp}{dz}. \tag{A1}$$

The solution for this equation for the case of a flow between large plates is given by Eq. (1). For the description of the rectangular pipe we insert in this equation a correction term $u(x_1,x_2)$:

$$v(x_1,x_2)=\frac{1}{2\eta}\frac{dp}{dz}\left[x_v^2-x_2^2+u(x_1,x_2)\right] \tag{A2}$$

and it is seen that for this correction term:

$$\nabla^2 u=0. \tag{A3}$$

Now the Laplace equation (A3) has to be solved. We require that the velocity v, as a function of the horizontal direction x_1 and the vertical direction x_2, at the boundary of the pipe is zero. This means that

$$u=x_2^2-x_v^2 \quad \text{on } x_1=\pm x_h \wedge u=0 \quad \text{on } x_2=\pm x_v. \tag{A4}$$

The solution is found using the method of separation of variables. This leads to

$$u(x_1,x_2)=\sum_{n=0}^{\infty} A_n \cosh c_n x_1 \cos c_n x_2. \tag{A5}$$

The coefficients A_n and c_n can be found by insertion of the boundary conditions. Using the orthogonality relation

$$\int_{-x_v}^{+x_v} \cos c_n x_2 \cos c_m x_2\, dx_2=\delta_{mn}, \tag{A6}$$

with δ_{mn} as the Kronecker delta, we obtain

$$c_n=\left(n+\frac{1}{2}\right)\frac{\pi}{x_v};\quad A_n=\frac{32(-1)^{m+1}x_v^2}{2(m+1)^3\pi^3\cosh c_n x_h} \qquad \text{(A7)}$$

by which Eq. (2) is obtained.

[a]W. E. Booij and A. de Jongh were undergraduate M. Sc. students at the time of writing the manuscript. F. F. M. de Mul was the supervisor.
[b]Corresponding author.

[1]W. E. Langlois, *Slow Viscous Flow* (Macmillan, New York, 1964), pp. 117–124.
[2]L. E. Drain, *The Laser-Doppler Technique* (Wiley, Chichester, 1980).
[3]F. Durst, A. Melling, and J. H. Whitelaw, *Principles and Practice of Laser-Doppler Anemometry*, 2nd ed. (Academic, London, 1981).
[4]J. M. Bessem, R. Booij, H. Godefroy, P. J. de Groot, K. Krisha Prasad, F. F. M. de Mul, and E. J. Nijhof (Eds.), Proc. 5th Intern. Conf. on "Laser Anemometry: Advances and Applications," Veldhoven, Netherlands, 23–27 August 1993 (SPIE—The International Society for Optical Engineering, Bellingham, 1993), Vol. 2052.
[5]R. H. Balansky and K. H. Wanser, "Laser-Doppler velocimetry using a bulk optic Michelson interferometer—A student laboratory experiment," Am. J. Phys. **61**, 1014–1019 (1993).
[6]H. W. Jentink, M. A. Helsdingen, F. F. M. de Mul, H. E. Suichies, J. G. Aarnoudse, and J. Greve, "On the construction of small differential Laser Doppler velocimeters using diode lasers," Int. J. Optoelectron. **4**, p. 405–414 (1989).

Nonlinear crosstalk in a multichannel fiber-optic communication system

Hong Shi,[a] Yan Lin,[b] Sean Carney I, Aaron Zygmunt, and John R. Thompson
Department of Physics, DePaul University, Chicago, Illinois 60614

(Received 6 December 1994; accepted 13 March 1995)

Nonlinear mixing between the longitudinal modes of multimode laser pulses is used to illustrate the effects of nonlinear crosstalk in multichannel communication systems. The results of the experiments are compared with a simple theoretical model that was described in a recent article. The article concludes with suggestions for experiments in nonlinear fiber optics for undergraduate and masters students. © *1995 American Association of Physics Teachers.*

I. INTRODUCTION

The nonlinear propagation of pulsed laser light through optical fiber is a topic of great importance to science and technology. The primary driving force behind research in nonlinear fiber optics is the potential (only partially realized to date) of fiber-optic communication systems to dramatically increase the speed of digital information transport over their electronic counterparts. Nonlinearity frequently places limitations on high speed optical communication systems; consequently, it is important to understand nonlinear optical processes in fiber.[1–6]

Frequency-division multiplexing (FDM) is one technique for increasing the speed of optical communication systems that is currently receiving much attention. A FDM system uses optical carrier waves of slightly different frequencies that travel through the same fiber to encode different signals. For example, two phone conversations might be multiplexed onto a common strand of fiber by using a separate laser with a different operating wavelength to optically encode each voice signal. At the output end of the fiber, a dispersive element (such as a grating) can be used to route each signal to the proper destination. Of course, one can multiplex more than two channels so that the information capacity of a single strand of fiber *seems* boundless.[3]

As you probably anticipated, nonlinearity will limit how many channels you can add to a FDM system. The different channels, which are supposed to be independent, can begin to interact because of the intensity dependence of the refractive index of the glass fiber. One bit (or pulse) modulates the index seen by another bit, which is equivalent to modulating its phase. This phase modulation leads to the production of sidebands which drain energy from the original carrier waves. The sidebands may also overlap with other carriers and interfere with them, leading to transmission errors.[2–5] The input and output spectra for a two channel FDM system when nonlinearity is important is shown in Fig. 1. Thus, in order to properly design a FDM communication system, we must understand about nonlinear crosstalk between different channels.

In this article we describe measurements that illustrate the nonlinear mixing that we have just outlined. These measurements are compared with a simple theoretical model for nonlinear propagation in fiber that was presented in a recent article.[1] Discrepancies between the measured and calculated

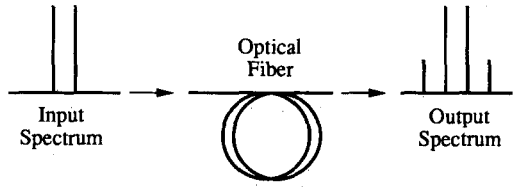

Fig. 1. Input and output spectra for a two channel FDM system illustrating the effects of nonlinear crosstalk.

